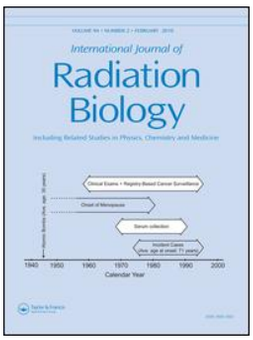

International Journal of Radiation Biology

ISSN: 0955-3002 (Print) 1362-3095 (Online) Journal homepage: https://tandfonline.com/loi/irab20

Development of a biodosimeter for radiation triage using novel blood protein biomarker panels in humans and non-human primates

Robert P. Balog, Rowena Bacher, Polly Chang, Michael Greenstein, Songeeta Jammalamadaka, Harold Javitz, Susan J. Knox, Shirley Lee, Hua Lin, Thomas Shaler, Lei Shura, Paul Stein, Kathryn Todd & David E. Cooper

To cite this article: Robert P. Balog, Rowena Bacher, Polly Chang, Michael Greenstein, Songeeta Jammalamadaka, Harold Javitz, Susan J. Knox, Shirley Lee, Hua Lin, Thomas Shaler, Lei Shura, Paul Stein, Kathryn Todd & David E. Cooper (2019): Development of a biodosimeter for radiation triage using novel blood protein biomarker panels in humans and non-human primates, International Journal of Radiation Biology, DOI: 10.1080/09553002.2018.1532611

To link to this article: https://doi.org/10.1080/09553002.2018.1532611

Published online: 03 Jan 2019.

INTERNATIONAL JOURNAL OF RADIATION BIOLOGY
https://doi.org/10.1080/09553002.2018.1532611

Taylor & Francis
Taylor & Francis Group

ORIGINAL ARTICLE

Development of a biodosimeter for radiation triage using novel blood protein biomarker panels in humans and non-human primates

Robert P. Balog[a], Rowena Bacher[a], Polly Chang[a], Michael Greenstein[a], Songeeta Jammalamadaka[a], Harold Javitz[a], Susan J. Knox[b], Shirley Lee[a], Hua Lin[a], Thomas Shaler[a], Lei Shura[b], Paul Stein[a], Kathryn Todd[a] and David E. Cooper[a]

[a]SRI International, Menlo Park, CA, USA; [b]Department of Radiation Oncology, Stanford University, Stanford, CA, USA

ABSTRACT

Purpose: In a significant nuclear event, hundreds of thousands of individuals will require rapid triage for absorbed radiation to ensure effective medical treatment and efficient use of medical resources. We are developing a rapid screening method to assess whether an individual received an absorbed dose of $\geq$2 Gy based on the analysis of a specific panel of blood proteins in a fingerstick blood sample.

Materials and methods: We studied a data set of 1051 human blood samples obtained from radiotherapy patients, normal healthy individuals, and several special population groups. We compared the findings in humans with those from irradiation studies in non-human primates (NHPs).

Results: We identified a panel of three protein biomarkers, salivary alpha amylase (AMY1), Flt3 ligand (FLT3L), and monocyte chemotactic protein 1 (MCP1), which are upregulated in human patients receiving fractionated doses of total body irradiation (TBI) therapy as a treatment for cancer. These proteins exhibited a similar radiation response in NHPs after single acute or fractionated doses of ionizing radiation.

Conclusion: Our work provides confidence in this biomarker panel for biodosimetry triage using fingerstick blood samples and in the use of NHPs as a model for irradiated humans.

ARTICLE HISTORY
Received 5 June 2018
Revised 4 September 2018
Accepted 22 September 2018

KEYWORDS
Radiation biodosimetry; blood biomarkers; human radiotherapy patient studies; immunoassays; point of care test

Introduction

The Biomedical Advanced Research and Development Authority (BARDA) is tasked with developing a point-of-care (POC) radiation biodosimeter that can be used to triage potentially exposed individuals following radiological and nuclear events. Modeling studies performed at the Lawrence Livermore National Laboratory (Buddemeier 2011, 2015) indicate that up to one million individuals will need to be triaged following a 10 kt nuclear event in either NYC or WDC. Such a triage device must be capable of distinguishing between absorbed doses of $<$2 Gy and $\geq$2 Gy, have high classification accuracy for samples obtained in the 1- to 7-d post-exposure time window, perform comparably across the US demographic range for all age groups, and not be confounded by common medical conditions prevalent in the US population or special population groups designated by the Department of Health and Human Services (DHHS). Additionally, the device should be operable by minimally trained individuals and provide a result in about 30 min from a fingerstick blood sample.

SRI International (SRI) is working to develop a POC biodosimeter capable of meeting these requirements. Our basic approach is to use a set of host-response plasma proteins that are indicative of exposure to ionizing radiation at or above a threshold level (which is 2 Gy in humans but likely different in an animal model). In a companion paper (Balog et al. 2018), we described results from three large-scale non-human primate (NHP) studies and identified a panel of protein biomarkers that are significantly elevated in NHPs in response to acute absorbed doses of ionizing radiation. These biomarkers included alpha-1-antichymotrypsin (AACT), alpha amylase (AMY), Fms-related tyrosine kinase 3 ligand (FLT3L), and monocyte chemotactic protein 1 (MCP1). We demonstrated this panel of biomarkers can classify a large data set of NHP blood plasma samples with high accuracy, and the baseline levels of these markers and subsequent levels following significant absorbed doses of radiation can be detected using a simple lateral flow test suitable for use in a POC device. An earlier paper (Bazan et al. 2014) discussed some of our initial work on proteins as useful radiation biomarkers in humans based on initial observations in patients undergoing radiotherapy. The current paper presents additional results from those patients and others in special population groups, compares results with those observed in NHPs, and identifies a specific panel of proteins useful for radiation biodosimetry. Here we show three biomarkers AMY1, FLT3L, and MCP1 are significantly upregulated in human radiotherapy patients receiving fractionated doses of ionizing radiation administered over a period of several days.

These three markers have all been previously reported in the literature in the context of radiation injury. Salivary alpha

CONTACT David E. Cooper david.cooper@sri.com SRI International, Room 30601, 333 Ravenswood Avenue, Menlo Park, CA 94025, USA
Color versions of one or more of the figures in the article can be found online at www.tandfonline.com/irab.
This article has been republished with minor changes. These changes do not impact the academic content of the article.

amylase (AMY1) is highly expressed in the salivary gland and known to be indicative of radiation injury to the parotid gland (Kishima et al. 1965). The rise in AMY1 from irradiation of salivary tissue provides a unique biochemical measure of early radiation effect in normal tissue (Guipaud and Benderitter 2009). Indeed, the post-irradiation increase in AMY1 is a good criterion for triage of accidentally irradiated patients and may be used as a biological dosimeter (Citrin et al. 2012) as well as in radiotherapy patients receiving total body irradiation (Barrett et al. 1982; Junglee et al. 1986). Early changes in salivary gland function are similarly marked in patients receiving either accelerated radiotherapy or conventional fractionated radiation treatment for some head and neck cancers (Guipaud and Benderitter 2009; Leslie and Dische 1992).

FLT3L is a hematopoietic cytokine that works in synergy with other growth factors to stimulate the proliferation and differentiation of various blood cell progenitors. Plasma FLT3L concentrations during the first 5 d of radiation therapy directly correlate with the radiation dose in an NHP model (Bertho et al. 2001). For patients receiving radio-immunotherapy, the FLT3L-adjusted red marrow radiation dose correlates with hematologic toxicity, and FLT3L is expressed following radiation-induced injury to the bone marrow (Kenins et al. 2008). Levels of FLT3L correlate with the severity of damage to major organ systems in victims accidentally exposed to ionizing radiation (Bertho et al. 2008, 2009).

MCP1 is a potent chemotactic factor for monocytes and is produced by a variety of cell types, either constitutively, or after induction by oxidative stress; it has been demonstrated to recruit monocytes into foci of active inflammation from infectious diseases (e.g. tuberculosis), rheumatologic diseases (e.g. rheumatoid arthritis), and cancers (e.g. breast cancer) (Deshmane et al. 2010). MCP1 levels have been observed in patients with non-small cell lung cancer (NSCLC) treated with radiation (60 Gy in 30 fractions over 6 weeks). The mean lung radiation dose correlated with a reduction in plasma levels of MCP1 1 h after irradiation. However, MCP1 concentrations at 4 weeks were increased in patients with severe pulmonary toxicity compared to those without severe toxicity (Siva et al. 2014). Ionizing radiation induced the expression of MCP1 in meningioma cell lines (Nalla et al. 2011), rat liver cells (Moriconi et al. 2008), and human lung endothelial cells (Gaugler et al. 2005).

Using a percentile classification algorithm described below, we used our panel of three biomarkers (AMY1, FLT3L, and MCP1) to classify a data set consisting of 1051 human samples with an accuracy of 92%, a sensitivity of 90%, and a specificity of 93%. This human data set consists of samples obtained from normal healthy individuals, several special population groups, and human radiotherapy patients who received fractionated doses of total body radiation. We also show the marker response in patients undergoing radiotherapy is similar to that observed in radiation-exposed NHPs.

Materials and methods

Human clinical studies

All human samples used in the present study were obtained with informed consent under an appropriate Institutional Review Board (IRB)-approved protocol. Samples from radiotherapy patients, individuals with traumatic injuries and infections, and healthy donors were obtained at the Stanford University Medical Center (SUMC). Samples from healthy donors and patients in several special population groups (i.e. those who were diabetic, obese, pregnant, or had compromised immune systems or rheumatoid arthritis) were obtained commercially from Bioreclamation. Samples from burn patients were obtained at the UC Davis Medical Center (UCDMC), and additional samples from immunocompromised patients were obtained from the Duke University Medical Center.

Radiotherapy patients

These patients were typically between 18 and 65 years old and undergoing treatment for leukemia or lymphoma. Patients were excluded from the study if they had received any chemotherapy within 21 d of radiation treatment or any prior radiation treatment. The most common treatment plan for patients undergoing total body irradiation (TBI) at the SUMC includes three doses of 1.2 Gy/day, with each dose separated by ~3 h for a period of 4 d. The TBI was delivered via 15-MV photons with two equally weighted beams (anterior–posterior/posterior–anterior) at a dosage rate of 0.13–0.17 Gy/min. Custom-tailored blocks were designed for each patient to provide 50% shielding of the lungs from X-rays. The bone marrow under the lung blocks then received an additional boost of radiation with 15-MV electrons. The electron energy was selected to deliver radiation to the depth of the chest wall, with as little as possible to the underlying heart and lungs.

A total of 232 samples were collected from 65 patients. The TBI blood samples were collected from all 65 patients (35M/30F) before treatment on day 1, from 60 of the patients (32M/28F) before treatment on day 2 (after three fractions totaling 3.6 Gy), from 60 of the patients (31M/29F) on day 3 (after six fractions totaling 7.2 Gy), and from 47 of the patients (24M/23F) on day 4 (after nine fractions totaling 10.8 Gy).

Control and special population groups

Samples were collected from both control and special population groups. The control group consisted of 272 (155M/117F) samples from healthy donors and included samples from 154 adults (age range 22–65 years), 61 adolescents (age range 12–21 years), and 57 geriatrics (age range >65 years). These samples were obtained from both SUMC and Bioreclamation and covered a demographic distribution representative of the US.

Additional blood samples were purchased from Bioreclamation and included 96 (50M/50F) type II diabetics, 88 (50M/38F) obese patients (BMI >30), 100 pregnant women, and 89 (44M/45F) rheumatoid arthritis patients. Blood samples from 53 (39M/14F) individuals with traumatic injuries and 61 (19M/42F) with mild infections were collected by SUMC. These individuals had experienced bone breaks, lacerations, knife and bullet wounds, or had upper

respiratory infections. Samples from 12 immunocompromised individuals (CD4 counts <200) were obtained from both Bioreclamation and Duke. A total of 48 samples obtained from 10 (9M/1F) burn patients were collected at multiple time points over a period of 1–7 d following admission to the UCDMC. Burn patients were included in the study provided they were 18 years or older and had no admission diagnosis other than a burn injury that included greater than or equal to 10% of total body surface area but less than or equal to 30%. All samples collected from these special population groups were collected at unspecified time points within each given clinical condition.

Blood collection

Venous blood was collected using a single BD™ P100 Blood Collection System for preservation of plasma proteins. Each tube was collected to the full 8-mL volume, inverted 8–10 times to thoroughly mix the P100 anticoagulant, and then placed inside a Ziploc bag on a layer of wet ice inside a Styrofoam container. Each P100 tube containing blood was centrifuged at 1600 g for 30 min. Using a 1000-µl micro pipettor with appropriately sized tips, 500-µl aliquots of plasma were transferred from the top layer in the P100 tubes into the appropriate number of individual screw-cap 1.5-mL microcentrifuge tubes. These aliquot tubes were stored at −80 °C until they were shipped on dry ice to SRI. All received samples were stored at −80 °C until analysis by mass spectroscopy or immunoassay. To minimize the effect of freeze-thaw cycles for analysis, samples typically were frozen for several months before analysis and underwent a single freeze-thaw cycle. An analysis in our laboratory of the effect of freeze-thaw cycles on analytical performance of our immunoassay demonstrated that samples remained stable for at least five freeze-thaw cycles. Also, plasma calibration samples stored for many months at −80 °C remained stable.

NHP studies

The NHP (*Macaca mulatta*) samples were obtained from several different irradiation studies as described in more detail elsewhere (Balog et al. 2018). These consisted of three large acute TBI exposure studies performed at CitoxLab (Montreal, Canada) and Lovelace Biomedical and Environmental Research Institute (LBERI) (Albuquerque, NM). The total NHP acute exposure sample set obtained from all three studies consists of 895 samples from healthy (baseline) NHPs as well as those receiving absorbed doses of radiation in the range of 1–10 Gy in whom blood was collected on days 1–7 following exposure. Each dose group contained 10 (5M/5F) animals (aged ~4 years). The use of animals and the study protocols were approved by the Institutional Animal Care and Use Committee (IACUC) in all participating institutes and by the sponsor.

Two other NHP irradiation studies were conducted at LBERI that included both acute and fractionated exposures. Animals received either single acute, double, or triple fractionated doses of 6-MV X-rays from a Varian 600c LINAC at a dose rate of 0.5–0.8 Gy/min. The single acute dose irradiation was delivered in a bilateral scheme with half of the dose to each of the left and right lateral sides. Fractionated doses were administered to a single side of each animal, and the side was alternated between doses.

The two fractionated dosing schemes were used to mimic common human TBI protocols. Each fractionated dosing scheme used 12 animals (6M/6F). In the first scheme, two 1.5 Gy dose fractions were administered per day; in the second scheme, three 1.2 Gy dose fractions were given per day. The dose fractions were administered on four consecutive days beginning on day 0 resulting in total cumulative doses of either 3, 6, 9, and 12 Gy or 3.6, 7.2, 10.8, and 13.2 Gy on days 1, 2, 3, and 4 for the double and triple fractionated dose schemes, respectively. Blood samples were collected from each animal on days −3, 1, 2, 3, 4, and 7 with collection times corresponding to cumulative doses of 0 Gy (day −3), 3 Gy (day 1), 6 Gy (day 2), 9 Gy (day 3), and 12 Gy (days 4 and 7) in the animals receiving double fractionated doses and cumulative doses of 0 Gy (day −3), 3.6 Gy (day 1), 7.2 Gy (day 2), 10.8 Gy (day 3), and 13.2 Gy (days 4 and 7) in the animals receiving triple fractionated doses. The single acute exposure groups in this study consisted of 3 animals (2F/1M) receiving a single dose of 12 Gy and 4 animals (2M/2F) receiving a single dose of 13.2 Gy.

In the second study, two groups of eight animals (4M/4F) received a single acute dose of either 3 Gy or 3.6 Gy and an additional two groups of eight animals (4M/4F) received doses of 3 Gy or 3.6 Gy administered in two fractions of 1.5 Gy or three fractions of 1.2 Gy. All animals were irradiated on day 0 and blood samples were collected from each animal days -3, and days 1, 2, 3, 4, and 7 post-irradiation.

Immunoassays

Immunoassays were performed in duplicate with a conventional enzyme-linked immunosorbent assay (ELISA) in a sandwich format on the human samples for six different protein targets – AACT, AMY1, FLT3L, IL15, MCP1, and NGAL – using commercially available kits. Each assay plate included one or more plasma sample standards to evaluate assay variability. For all assays, the inter-plate coefficients of variation (CVs) ranged from 2.3% to 14%.

As described elsewhere (Balog et al. 2018), immunoassays conducted on the NHP samples were performed in duplicate with conventional ELISA in a sandwich format for the same six protein targets as for the human samples. Each assay plate included one or more plasma sample standards to evaluate assay variability. For all NHP assays, the inter-plate CVs ranged from 3.6% to 11.7%, with an average CV of 10%.

Statistical methods

We analyzed the data using the comprehensive statistical analysis package known as *R*, which is available as freeware and widely used within the biostatistics community, the Matlab Statistics toolpack, and the Stata statistical and data analysis software. Initial data processing consisted of reading

in the raw data files produced by the ELISA instrument and preparing a master data file consisting of Excel spreadsheets of the data for each protein for each plasma sample. Standard analyses included preparing boxplots, histograms, assay CVs, correlation tables, and fold-change plots for each protein. Most analyses were performed on log-transformed data because it was more normally distributed than the untransformed data. Both paired and unpaired *t*-tests were performed as well as linear regressions to identify proteins that changed significantly from baseline as a result of irradiation. Data sets were classified using several supervised classifiers that included logistic regression, support vector machine, and conditional inference trees.

We also used a new classification method developed at SRI, which we refer to as the percentile classification algorithm (PCA). Although results were similar using all of the classifiers, the percentile classification approach compares the biomarker concentration from an unknown sample against the distribution of concentrations for normal individuals for that biomarker. The result of this comparison is a value *p*, which is the proportion of normal healthy subjects that have a biomarker concentration greater than that measured in the unknown sample. We call this value the "upper tail probability" for the biomarker of the unknown sample. This process is repeated for all biomarkers in a panel, and a test statistic (TS) is obtained by summing $-\ln(p)$ for each biomarker.

The TS value obtained from the unknown sample is then compared against a threshold value to determine whether the test result is positive or negative. The threshold value for the TS was obtained from observations of normal individuals not exposed to radiation and set to yield a false-positive rate (FPR) of 5% (or equivalently, 95% of normals have a TS that lies below this threshold). Empirically, we find this works well for both our human and NHP data sets, and it can be varied if one desires to have a lower false-negative rate (FNR) at the expense of a higher FPR. This is similar to Fisher's method of combining probabilities (Fisher 1925) and offers several advantages for our application using a panel of biomarkers: (1) it is based only on the distribution of normals, so no data from irradiated individuals or animals is required; (2) it is scalable from a single biomarker to many biomarkers; (3) for normalized and standardized data sets, the algorithm is species independent for humans and NHPs; and (4) there are no assumptions regarding dose equivalence between humans and NHPs. In our analyses, all data were first log-transformed and then the mean and standard deviation for each transformed protein were calculated for normal healthy subjects. Our data sets were then standardized by subtracting the mean concentration for normals from each measured value for each protein and dividing by the standard deviation for normals. This procedure was performed separately for each species. Results from these analyses are presented in the following sections.

Results

Immunoassay

Figure 1 shows the boxplots for the human data sets for the proteins AACT, AMY1, FLT3L, IL15, MCP1, and NGAL for the control, special population, and TBI groups (for non-standardized, non-normalized data). Due to the relatively large variation in protein concentrations, the log10 of the protein concentration (in ng/mL) is plotted.

We also conducted t-test comparisons of the various human confounder groups against the control group using the ELISA data obtained from analysis of human plasma samples (Table 1). For each group, the table shows whether a protein of interest is higher (red up-arrow) or lower (green down-arrow) as compared to the controls. A red or green arrow indicates the p-value is less than 0.05 and, therefore, likely to be statistically significant. To correct for multiple comparisons, we applied the Bonferroni correction factor to each *p*-value to ensure there was no more than a 5% probability of any false statistically significant results across all tests. Although for any given protein there are differences between some of the special population groups and controls, none of the special groups exhibited a pattern for the five proteins of interest (AACT, AMY1, FLT3L, NGAL, and MCP1) that was similar to that observed in the radiotherapy patients. Table 2 lists the mean plasma concentrations (in ng/mL) and the 95% confidence intervals for each human subgroup for the proteins AMY1, FLT3L, MCP1, AACT, NGAL, and IL15 as measured by ELISA. The red boxes in the table highlight the mean concentrations observed in the human radiotherapy patients for each biomarker. For the markers AMY1, FLT3L, and MCP1, we observed mean values that increased with absorbed radiation dose in these patients. No significant change was observed for AACT, the NGAL levels dropped, and the boxplot for IL15 shows a slight increase with increasing absorbed dose.

For AACT, the boxplot in Figure 1 indicates this protein is not radiation responsive in human TBI patients because there was no significant change in the levels of this protein compared to controls. Conversely, in NHPs AACT appeared to be strongly radiation responsive and increased with increasing absorbed dose (Balog et al. 2018). It is not clear why the radiation response of the AACT is so different between the human TBI patients and NHPs. The AACT levels in the trauma and burn patient groups increased relative to the control group. The *t*-test results in Table 1 and the mean plasma concentrations in Table 2 reflect these results. The levels of AACT in the TBI patients were not statistically significantly different from levels in the control group. The trauma and burn subgroup *p*-values were statistically significant.

The mean AMY1 levels in the TBI patient subgroup were significantly increased relative to controls and same-subject exposure before radiation. No clinical evidence of parotitis was observed in the TBI patients indicating that the increased plasma levels of AMY1 were due to radiation damage to the parotid gland rather than radiation-induced inflammation. The AMY1 levels increased significantly above baseline (p values $< .0001$) and dropped at the highest dose (although were still well above baseline). The *t*-test results in Table 1 show several other subgroups (pregnant women, and those with rheumatoid arthritis) had mild AMY1 level elevations relative to the controls. However, as can be seen in the boxplot and in Table 2, these elevations were far

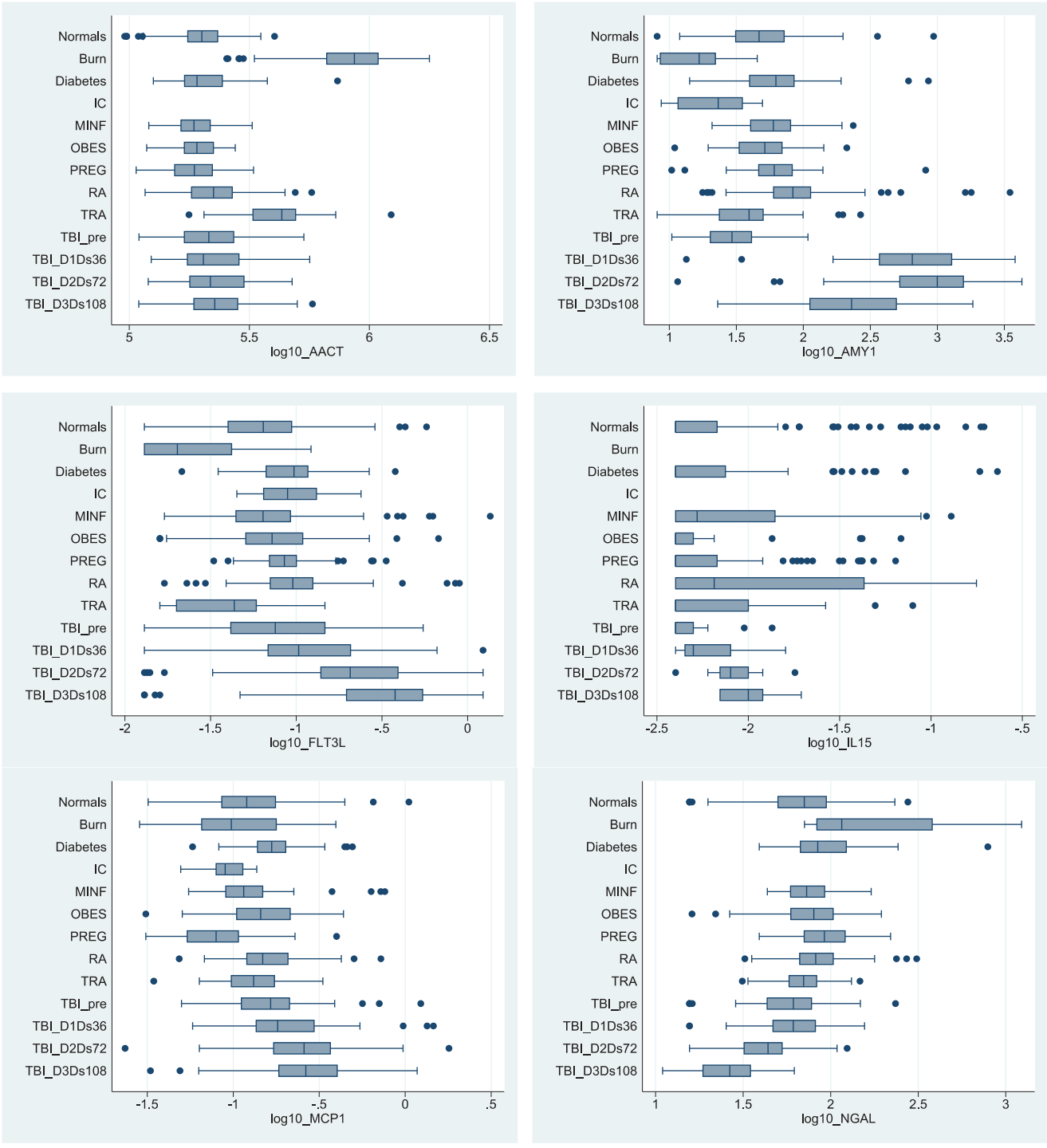

Figure 1. Boxplots for human data sets for AACT, AMY1, FLT3L, IL15, MCP1, and NGAL. The horizontal scale for all plots in the log10 of the measured plasma concentration in ng/mL. The TBI data was obtained from radiotherapy patients who had received three dose fractions of 1.2 Gy per day administered over three consecutive days. Individuals were irradiated on day 0 and whole blood samples were collected on days 0, 1, 2, and 3 at which time the patients had received cumulative doses of 0, 3.6, 7.2, and 10.8 Gy.

below those observed in the post-exposure radiotherapy patients. The AMY1 levels in burn and pre-exposure TBI patients were lower than those observed in the controls.

The FLT3L boxplots of post-exposure TBI patients show their plasma levels were significantly more elevated than in controls, and the levels increased with increasing dose and an increasing timepoint following exposure. The FLT3L levels in those in other subgroups were comparable to controls (see *t*-test table, Table 1). The post-exposure TBI patients exhibited elevated FLT3L levels relative to the controls ($p < .0001$). The low FLT3L levels observed in the burn and trauma patients were statistically significant ($p < .0001$) compared to healthy human controls. The elevated levels of FLT3L observed in the diabetic and arthritic individuals were well below that observed in the post-exposure TBI patients (Table 2).

The MCP1 levels increased with absorbed dose in the TBI patients versus controls ($p < .0001$). Some samples from the

Table 1. *t*-Test results from the human data sets.

GROUP versus CTRL	AACT	AMY1	FLT3L	MCP1	NGAL	IL15
BURN	↑(<1e-4)	↓(<1e-4)	↓(<1e-4)	—	↑(.007)	
DIEB	—	—	↑(<1e-4)	↑(<1e-4)	↑(<1e-4)	—
MINF	—	—	—	—	—	—
OBES	—	—	—	—	—	—
PREG	—	↑(.002)	↑(<1e-4)	↓(<1e-4)	↑(<1e-4)	—
RA	—	↑(<1e-4)	↑(<1e-4)	↑(.005)	↑(.009)	—
TRA	↑(<1e-4)	—	↓(<1e-4)	—	—	—
TBI-Pre	—	↓(<1e-4)	—	↑(.03)	—	—
TBI-D1Ds3.6	—	↑(<1e-4)	↑(<1e-4)	↑(<1e-4)	—	—
TBI-D2Ds7.2	—	↑(<1e-4)	↑(<1e-4)	↑(<1e-4)	↓(<1e-4)	—
TBI-D3Ds10.8	—	↑(<1e-4)	↑(<1e-4)	↑(<1e-4)	↓(<1e-4)	—

Arrows indicate the resulting *p* value was statistically significant (<.05). Red and green arrows indicate protein levels are higher or lower relative to the control group. The numbers in parentheses are the resulting *p* values. The results were obtained on log10 transformed data using the Bonferroni correction for multiple comparisons. The TBI results are separated into subsets denoted by time point and total dose. For example, d1ds360 means day 1 samples with total cumulative dose of 3.6 Gy.

other subgroups exhibited levels comparable with the control group; however, in those with diabetes or rheumatoid arthritis, MCP1 levels were well below those observed in the TBI patients (Table 2). Pregnant women had MCP1 levels below those observed in the controls. Before radiation, MCP1 levels were elevated in the TBI patients relative to the controls ($p = .03$) (Table 2); following TBI, their mean MCP1 plasma concentrations were well above baseline levels.

We have IL15 levels for only about half the number of individuals in each subgroup (and no IL15 data for those who had burns or were immunocompromised); the boxplot shows plasma levels increased slightly in the post-exposure TBI patients, but *t*-test results indicate no statistically significant differences between the TBI post-exposure subgroup and the controls. Conversely, in NHPs, the IL15 levels were strongly radiation responsive and increased with higher absorbed doses (Balog et al. 2018). Again, it is not clear why the radiation response of this marker is different in humans and NHPs.

The boxplot shows plasma levels of NGAL decreased with radiation exposure. The *t*-test results confirmed this and showed samples from subgroups of those who had burns, were diabetic, pregnant, or had rheumatoid arthritis all exhibited elevated levels of NGAL relative to the controls.

Three proteins, AMY1, FLT3L, and MCP1, provided a unique descriptor of radiation exposure in human TBI patients (Table 1) and were significantly elevated in response to absorbed doses of radiation (except in patients with rheumatoid arthritis, in whom these markers appear to be elevated relative to controls); thus, our classifier exhibits a higher FPR in these subjects than in controls). Inclusion of either IL15 or NGAL or both in our panel does not improve our classification results. Furthermore, both IL15 and NGAL are more challenging to measure at clinically relevant levels than the markers in our panel.

Table 2 provides some insight into the natural variability of each of our protein markers in the normal and special population groups and how this variability compares with the observed increases in the levels of these proteins in

Table 2. Mean, upper, and lower 95% confidence bounds for biomarker concentrations (in ng/mL) for each human subgroup.

		AMY1			FLT3L			MCP1			AACT			NGAL			IL15		
Group	N	Mean	LCB	UCB	Mean	LCB	UCB	Mean	LCB	UCB	Mean	LCB	UCB	Mean	LCB	UCB	Mean	LCB	UCB
Normals	272	**58.3**	50.6	65.9	**0.076**	0.069	0.083	**0.148**	0.136	0.160	**205786.4**	200185.8	211387.0	**76.19**	71.61	80.76	**0.016**	0.010	0.022
Burns	48	**17.3**	14.8	19.7	**0.035**	0.026	0.043	**0.133**	0.106	0.160	**849813.8**	751201.2	948426.4	**320.94**	163.54	478.34			
Diabetics	96	**80.8**	60.0	101.6	**0.100**	0.090	0.110	**0.181**	0.167	0.196	**212872.2**	197407.3	228337.1	**103.29**	86.86	119.72	**0.014**	0.007	0.022
Mild Infection	61	**67.9**	57.4	78.4	**0.126**	0.075	0.177	**0.151**	0.116	0.186	**192643.1**	182299.6	202986.6	**78.10**	71.58	84.63	**0.017**	0.010	0.025
Obese	88	**55.7**	49.4	62.0	**0.091**	0.074	0.109	**0.172**	0.153	0.192	**195858.2**	188274.6	203441.8	**85.35**	77.72	92.98	**0.009**	0.004	0.015
Pregnant	100	**73.3**	57.7	89.0	**0.092**	0.083	0.101	**0.087**	0.077	0.096	**189790.6**	181403.3	198177.9	**98.49**	91.34	105.64	**0.009**	0.007	0.011
Rheumatoid Arthritis	89	**178.0**	87.5	268.4	**0.130**	0.100	0.160	**0.175**	0.155	0.194	**236547.9**	220203.9	252891.9	**91.11**	81.82	100.40	**0.030**	0.018	0.042
Trauma	53	**49.9**	37.4	62.4	**0.046**	0.038	0.053	**0.143**	0.125	0.161	**431183.5**	385006.3	477360.7	**74.35**	68.12	80.58	**0.011**	0.005	0.018
Immune Compromised	12	**24.9**	17.0	32.8	**0.109**	0.073	0.145	**0.094**	0.077	0.110									
TBI-0 Gy	65	**36.6**	30.6	42.7	**0.113**	0.086	0.139	**0.198**	0.157	0.240	**235694.1**	214039.1	257349.1	**65.81**	57.10	74.51	**0.005**	0.004	0.006
TBI-3.6 Gy	60	**942.0**	735.4	1148.5	**0.168**	0.121	0.215	**0.268**	0.203	0.334	**236799.1**	213268.9	260329.3	**66.64**	58.62	74.67	**0.006**	0.005	0.008
TBI-7.2 Gy	60	**1217.6**	972.0	1463.1	**0.278**	0.218	0.337	**0.313**	0.247	0.380	**242931.1**	221065.1	264797.1	**45.14**	39.76	50.53	**0.009**	0.007	0.010
TBI-10.8 Gy	47	**344.3**	250.1	438.5	**0.394**	0.322	0.467	**0.323**	0.257	0.389	**248380.3**	221793.5	274967.1	**27.79**	24.41	31.18	**0.011**	0.008	0.013
NHP-0 Gy	391	**1043.5**	1006.4	1080.6	**0.079**	0.076	0.082	**0.161**	0.155	0.168	**112263.7**	108268.4	116259.0	**0.023**	0.019	0.026			
NHP-3.6 Gy	20	**6301.6**	3676.2	8927.0	**0.106**	0.092	0.120	**0.487**	0.380	0.593	**398410.7**	369194.4	427627.0	**109.67**	93.55	125.78			
NHP-7.2 Gy	6	**2024.4**	728.1	3320.8	**0.143**	0.104	0.181	**0.914**	0.581	1.247	**394237.0**	319864.3	468609.7	**74.56**	53.29	95.83			
NHP =10.8 GY	6	**2058.4**	1702.7	2414.1	**0.389**	0.333	0.445	**1.443**	1.016	1.870	**321609.1**	285385.7	357832.5	**78.93**	65.19	92.67			

N is the number of subjects in each group[a]. The red boxes highlight the mean values observed in human radiotherapy patients. For comparison purposes we have included the mean, upper, and lower 95% confidence bounds for NHPs that underwent the same fractionated exposure protocols as the human TBI patients.
[a]AACT, NGAL, and IL15 data are unavailable for the immunocompromised patients. The IL15 values are not available for the burn patients and are only available for about half of the individuals in each other subgroup.

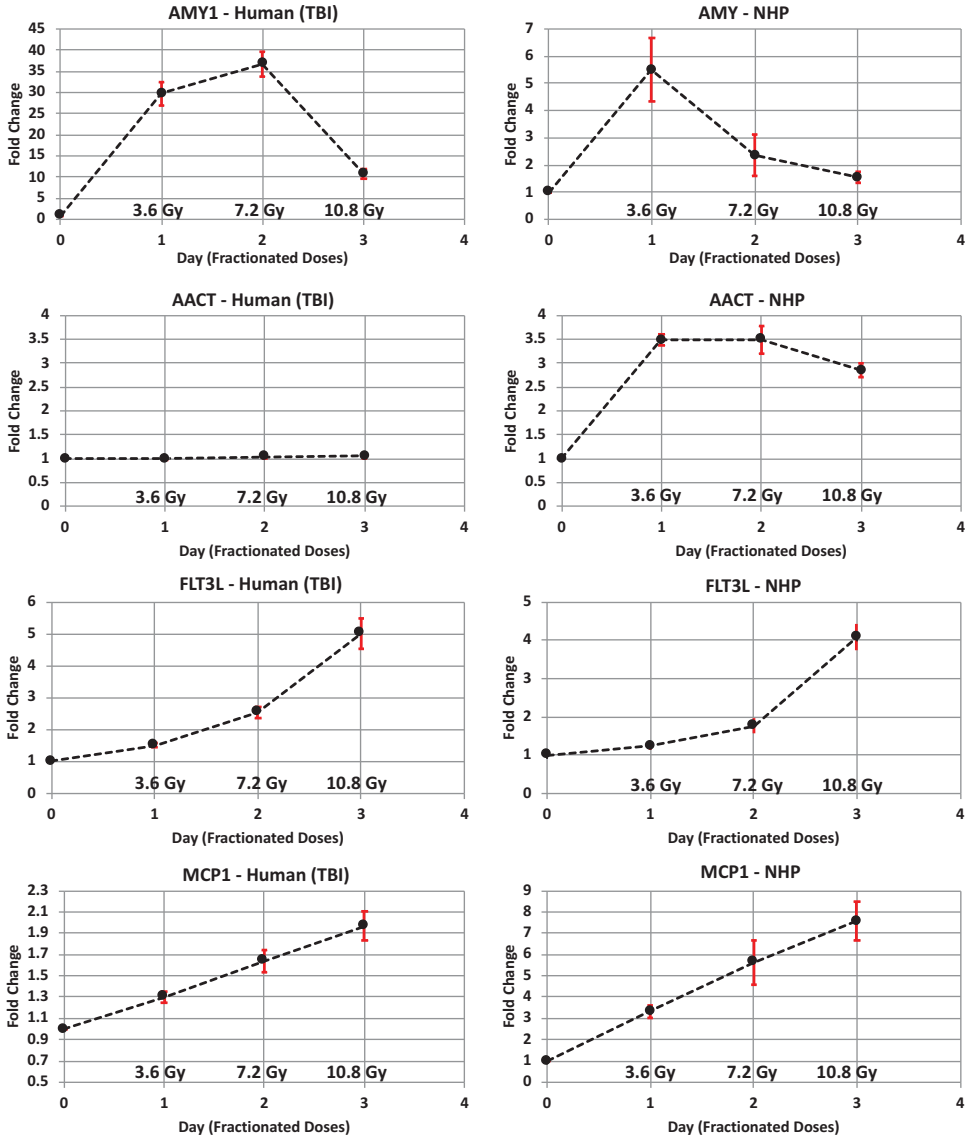

Figure 2. Fold-change plots for human TBI patients (top) and NHPs (bottom) for the four protein markers AMY1, AACT, FLT3L, and MCP1 following identical fractionated dosing of 1.2 Gy administered 3× per day. Samples collected on days 1, 2, and 3 were from subjects who received cumulative doses of 3.6, 7.2, and 10.8 Gy administered on the previous days. The error bars are ±1 SEM.

human TBI patients. As can be seen from the table, there is almost no overlap between the 95% confidence intervals for human TBI patients receiving a 3.6 Gy fractionated dose and the various non-irradiated human subgroups. For AMY1, the lower confidence bound (LCB) for the TBI patients given 3.6 Gy is 11× higher than the upper confidence bound (UCB) for human normals and 2.7× higher than the UCB for RA patients, who have the largest UCB of all the non-irradiated subgroups. For both MCP1 and FLT3l, the LCBs lie well above the UCBs for human normals and at or just above the UCBs for most of the other non-irradiated subgroups. FLT3L, in particular, shows a slight overlap in patients with mild infections, RA, and those who were immune-compromised.

Comparison of human and NHP data

Fold-change comparison for similar fractionated dosing

The plasma concentrations of the three biomarkers, AMY1, FLT3L, and MCP1, were upregulated in both humans and NHPs in response to ionizing radiation and generally increased with increasing cumulative absorbed dose. As mentioned previously, the AACT was upregulated in radiation-exposed NHPs but not in human TBI patients. Figure 2 compares the fold changes measured in human TBI patients and NHPs for these three proteins. The NHP fold changes were obtained from a study we performed in which the NHPs received the same fractionated dosing as the human TBI patients – namely three 1.2-Gy fractions per day for three consecutive days beginning on day 0 with sample collections on days 1, 2, and 3 following cumulative absorbed doses of 3.6, 7.2, and 10.8 Gy, respectively. In evaluating these data, it is important to note that cumulative dose and collection timepoint are not independent but confounded, that is the cumulative absorbed dose at each collection timepoint is different due to the fractionated protocol and therefore it is not possible from these data to determine the temporal kinetics of these biomarkers. For similar fractionated dosing protocols, the fold-change patterns were similar in both species

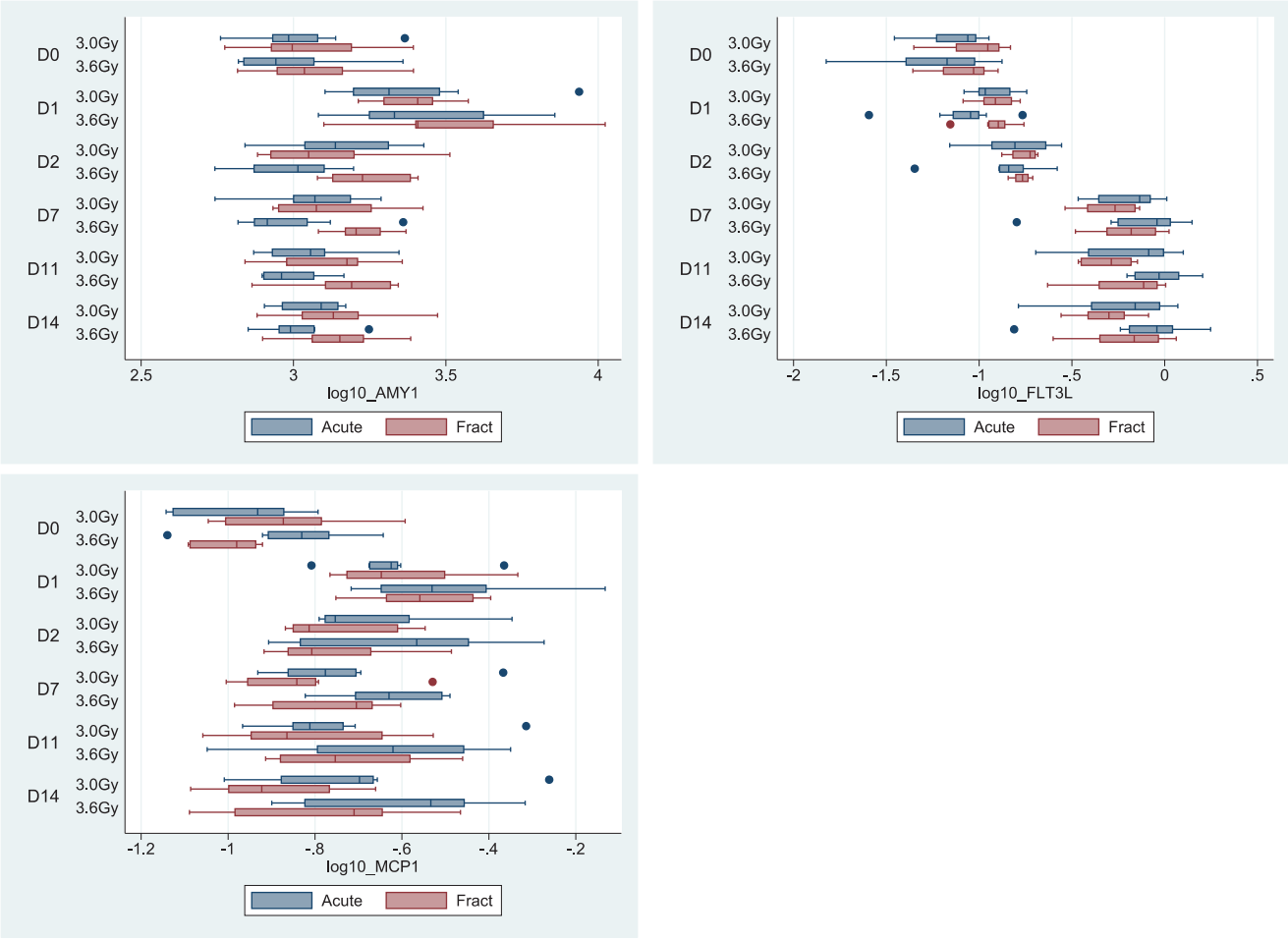

Figure 3. Fold-change plots for AMY1, FLT3L, and MCP1 in NHPs receiving single acute doses of 3 Gy and 3.6 Gy and double and triple fractionated doses of 3 Gy and 3.6 Gy. The differences observed between fractionated and acute dosing on each day were not statistically significant.

for both FLT3L and MCP1 although the magnitudes were different. For MCP1, the observed fold change is ~3× higher in NHPs than in humans. For FLT3L, the fold changes were comparable. For AMY, the kinetics appear to be different beyond the first day post-exposure and the fold change is significantly (5×–15×) higher in humans. Currently, we do not understand why, under a fractionated dosing schedule, the behavior of AMY1 appears to be different in NHPs and humans. As shown in the figure, human subjects show a stronger elevation in AMY1 levels as compared to NHPs, indicating this may be a better marker in humans rather than NHPs. Alpha amylase expression in NHPs may not be tissue specific as in humans – in NHPs it appears that alpha amylase is secreted by both the pancreas and the salivary glands and baseline levels are 10× higher than in humans. Although it appears from the graphs that AMY1 does not increase with dose, this is because the fractionated dosing schedule confounds dose and collection time. In NHP studies in which a single acute dose is administered (Balog et al. 2018), AMY levels do in fact increase with increasing dose, but AMY levels rapidly decrease back to baseline levels within 1 or 2 d.

Our classification algorithm does not rely on fold changes. Rather it computes the probability, *p*, that a normal subject would have plasma concentrations for each marker that are larger than the values observed in an unknown sample, and then sums up the logarithms of the *p* values. Therefore, the algorithm is not particularly sensitive to the magnitudes of the fold changes provided they are larger than the natural variations in biomarker concentration. Thus, we find our classifier works equally well for both NHPs and humans irrespective of the differences in fold change and kinetics between the two species.

NHP acute/fractionated dosing comparison

t-Test comparisons of the biomarker levels of interest in NHPs following an acute cumulative dose administered on a single day versus the same total fractionated dose (Figure 3) were not statistically significantly different. A permutation test, in which 1000 iterations assigned animals randomly to various exposure groups, was also performed and confirmed the *t*-test results. However, there were only eight animals (4M/4F) in each dose group, and this result should be considered preliminary. Future studies comparing fractionated and acute dosing protocols should contain sufficient additional animals to place an acceptable lower bound on the sensitivity and specificity of the assay.

Table 3. Classification summary using the three-biomarker panel for all human subgroups.

	% Positive (humans)							
	Dose (Gy)							
	0		3.6 (day 1)		7.2 (day 2)		10.8 (day 3)	
Group	*N*	%	*N*	%	*N*	%	*N*	%
Normals	272	4.8						
Burn	48	0.0						
Diabetics	96	9.4						
Mild infection	61	13.1						
Obese	88	6.8						
Pregnant	100	4.0						
Rheumatoid arthritis	89	21.3						
Trauma	53	0.0						
Immune compromised	12	0.0						
TBI-fract	65	9.2	60	90	60	95	47	85
Total *N*	**884**		**60**		**60**		**47**	
% Positive		**7.4**		**90**		**95**		**85**

At absorbed TBI doses ≥3.6 Gy, a large percentage of the observations are called as positives. *N* is the total number of subjects in each subgroup with the exception of the burn patients (48 samples were obtained from 10 burn patients).

Table 4. Classification results obtained from all human samples using the three-biomarker panel.

	Condition negative	Condition positive
Predicted negative	819	16
Predicted positive	65	151
Total	884	167

The corresponding sensitivity and specificity values are 90.4% and 92.6%, respectively.

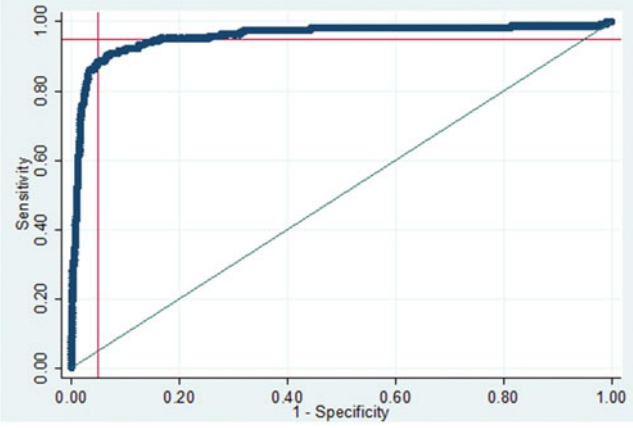

Figure 4. The ROC curve for all 1051 human normals, the confounder group, and TBI patient samples. The vertical and horizontal lines demark 95% sensitivity and specificity. The total AUC is 0.96 with 95% confidence bounds of 93.6% and 97.8%.

Classification of human data sets

Table 3 shows the percentage of observations classified as positive using our three-biomarker panel and percentile classification algorithm. At baseline, the FPR was 4.8% in normals. Overall, the FPR was 7.4%, and this includes those in the special population groups, which are over-represented in this study compared with the US population. Observed error rates were slightly higher than baseline rates for individuals with diabetes (9.4%) and obesity (6.8%) and significantly higher for those with rheumatoid arthritis (21.3%) or who had mild infections (13.1%). Before radiation exposure, TBI patients had an FPR of 9.2%. Following TBI, the FNRs were 10%, 5%, and 15% for individuals who received cumulative fractionated doses of 3.6, 7.2, and 10.8 Gy, respectively.

Inclusion of either IL15 or NGAL or both in our panel did not improve classification accuracy and reduced the sample set by approximately half because IL15 was only measured in about half of human samples. Including both proteins in our panel reduced the data set to 508 samples with an AUC of 0.995, an FPR of 6.7%, and an FNR of 0%. Classification of the same 508-sample set with our three-biomarker panel yielded an AUC of 0.997, an FPR of 5.9%, and an FNR of 0%.

Table 4 summarizes the performance of our classification scheme and three-biomarker panel on all human subjects. From the table, we infer an overall sensitivity of 90.4% and a specificity of 92.6% corresponding to an FNR of 9.6% and an FPR of 7.4%. The corresponding ROC curve is shown in Figure 4 (AUC = 0.96).

Cumulative distribution functions of human and NHP data sets

The cumulative distribution function (CDF) is a useful tool for evaluating and comparing the various human and NHP data sets. The CDF plots for each protein and the composite sum for human normals and TBI patients are shown in Figure 5. In this figure, the AMY1 exhibits the largest shift to the right from the normal distribution in human TBI patients and therefore has the strongest radiation response of the three markers. The MCP1 exhibits the smallest shift from the normal distribution and therefore has the weakest response of the three proteins.

Figure 6 shows CDFs of the test statistic (TS) values (sum of $-\ln(p)$) for human normals, those who received 0, 3.6, and 7.2-Gy fractionated TBI, and the 95% threshold level for the normal CDF plot. The CDF plot shows increasingly large shifts to the right for higher exposures. Similar trends were seen in the equivalent NHP CDF plots.

Comparison of human and NHP CDFs

Figure 7 plots the CDFs for both unexposed humans and NHPs and human TBI patients and healthy (baseline) NHPs receiving a total fractionated dose of 3.6 Gy or single acute doses of 3 and 4 Gy. The calculation of the composite biomarker CDF was performed independently in humans and NHPs. The NHP data covers the 1- to 7-d radiation post-exposure time window; however, the human data is not averaged over a full 1–7 d because it is based on the specific TBI therapeutic protocol used in which each cumulative dose is sampled at only a single time point. The CDFs for baseline human and NHP data are nearly identical; thus, species-normalized data inputs yielded comparable results.

As before, the curves shifted to the right with increasing absorbed radiation dose providing excellent discrimination between exposed and unexposed subjects for both species.

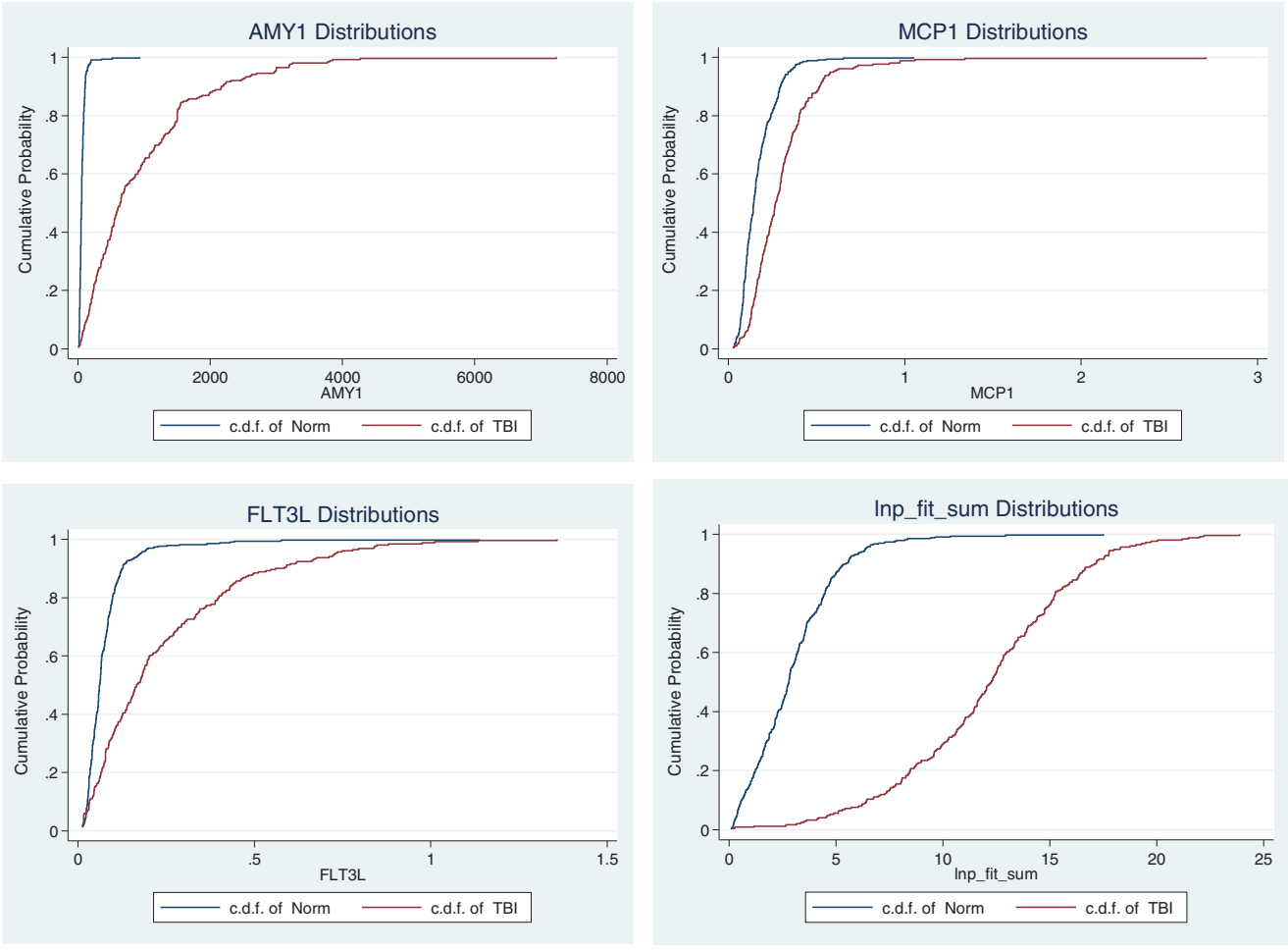

Figure 5. The CDF plots for human normals and post-exposure TBI patients for the proteins AMY1, FLT3L, and MCP1. The first three plots are for each individual protein. The last plot is the distribution obtained using all three proteins.

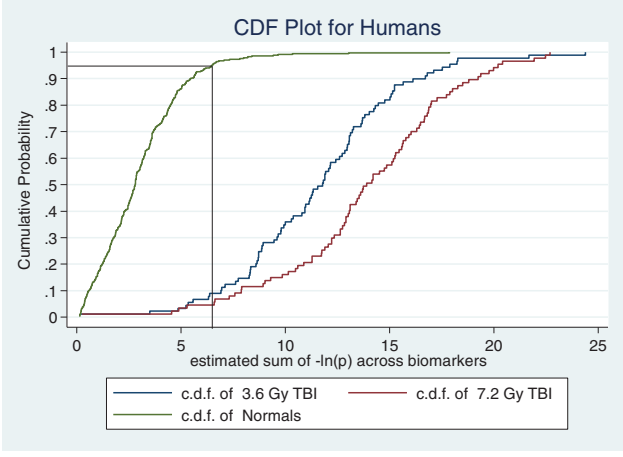

Figure 6. A CDF plot of cumulative probability versus the sum of $-\ln(p)$ across all of the biomarkers for human normals and TBI patients exposed to 3.6 and 7.2 Gy. The horizontal line is at the 95% percentile of the cumulative distribution, and the vertical line intersects the *x*-axis at the threshold for predicting whether an observation is from an individual exposed to $\geq$2 Gy.

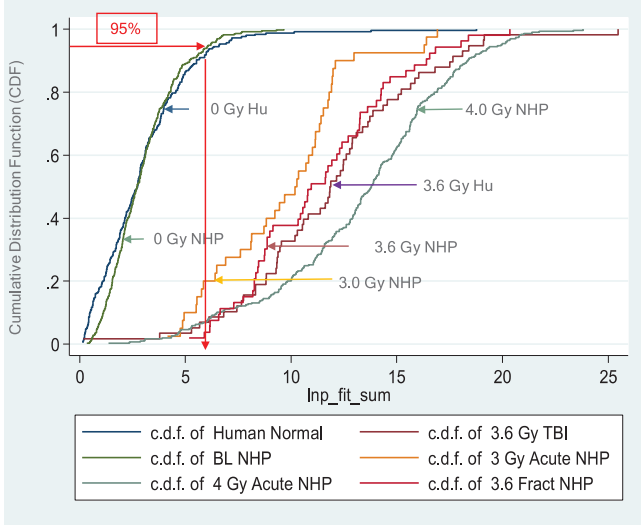

Figure 7. The CDFs for unexposed humans and NHPs, human TBI patients and healthy NHPs receiving a total fractionated dose of 3.6 Gy, and healthy NHPs receiving single acute doses of 3 and 4 Gy.

The CDFs for 3.6-Gy fractionated doses in NHP and human subjects receiving TBI are nearly identical, and the CDFs for the 3- and 4-Gy acute treatments in NHPs nicely bracket the 3.6-Gy curves following fractionated treatments. We conclude the results of an acute absorbed dose of ionizing radiation in NHPs are likely predictive of the response in healthy humans following acute exposure. Changes in our biomarker panel were similar in humans and NHPs following acute and fractionated radiation exposures.

Discussion

A rapid screening test is needed to guide effective use of medical resources in the aftermath of a nuclear event. Such a test will assess exposure and help determine the need for medical care or further evaluation with a more quantitative test that assesses actual absorbed dose. Modeling studies conducted by the US government indicate that hundreds of thousands to a million individuals will need to be triaged, and this will be most effectively carried out using a rapid screening assay.

The present study is directed toward development of such a rapid screening test. Our test is designed to rapidly assess whether or not an individual has received an absorbed dose at or above 2 Gy from a fingerstick blood sample. We note that several accurate gene expression assays have been developed to determine actual absorbed dose (Dressman et al. 2007; Port et al. 2018), and these assays are an important next step to direct more a patient-specific course of medical treatment. However, it is impractical to use such tests for rapid screening of a large number of individuals following a major nuclear event.

Because it is unethical to conduct irradiation studies in healthy humans, developing biomarkers useful for radiation biodosimetry must be based on data in humans undergoing radiation treatment for disease as well as data from animal models – particularly NHPs. Human radiotherapy patients have serious blood diseases and have received complex and profound drug treatments that may affect their responses to ionizing radiation. Furthermore, their treatment regimens do not ideally bracket the 2-Gy absorbed dose threshold, they receive fractionated doses administered over several days, and their samples are not obtainable over the full 7-d post-exposure time window of interest. Thus, they are not an ideal model and yet are the only reliable source of blood samples from individuals with known radiation exposure and must be included in studies of radiation biodosimetry.

We have shown three protein biomarkers, AMY1, FLT3L, and MCP1, are similarly elevated in the blood of both human radiotherapy patients receiving fractionated doses and in otherwise healthy NHPs receiving either single acute or fractionated doses of total body radiation.

This panel of three biomarkers can be used in an algorithm to classify a large human data set that includes radiotherapy patients, normal healthy individuals, and human subjects from special population groups (i.e. those with arthritis, diabetes, obesity, who were pregnant, immune-compromised, or had burns, traumatic injury, or mild infections) with high accuracy and relatively low error rates. The fact that these three markers allowed us to classify radiation exposure in both human and NHP data sets gives us confidence that the panel will work for healthy humans exposed to high levels of radiation. Our work suggests that studies in NHPs provide an excellent model for the expected radiation response in humans.

While the fold changes between normals and irradiated humans and NHP are impressive, variability can also be characterized by the degree of overlap of the biomarker distributions of these different groups, with less overlap being more desirable. The degree of overlap varies from day to day as

Table 5. Potentially confounding diseases, estimated prevalence and fold change for each biomarker used in the biodosimetry panel.

Protein biomarkers	Potentially Confounding Disease (Ingenuity Database)/Estimated US Prevalence (CDC, 2013)/Measured Fold Change (by SRI)								
Salivary Alpha Amylase (**AMY1A**)	Disease	Thyroid cancer	Rheumatoid arthritis	Diabetes	Trauma	Parotitis (Mumps, SA, MTB, HIV)	Sarcoidosis	Obese	
	Prevalence	<0.014%	~0.4%	9%	n/a	~0.0001%	<0.04%	>20%	
	Fold Change	~2×	2.5×	1.2×	0.73×	n/a	n/a	0.77×	
Fms-related tyrosine kinase 3 ligand (**Flt3L**)	Disease	Leukemia/melanoma	Rheumatoid arthritis	Diabetes	Trauma	Infection	Autoimmune thyroiditis Tx	Melanoma	
	Prevalence	<0.02%	~0.4%	9%	n/a	~1.4%	<0.5%	~0.02%	
	Fold Change	n/a	1.3×–2.0×	1.1X	0.48×	1.4×	n/a	n/a	
Monocyte chemoattractant protein-1 (**MCP-1**)	Disease	Breast/pancreatic cancer	Rheumatoid arthritis	Diabetes	Trauma	Infection	Inflammatory bowel	Hyper cholesterolemia	
	Prevalence	0.012%/<0.01%	~0.4%	9%	n/a	~1.4%	~2–10%	50%	
	Fold Change	n/a	1.6×	1.0×	0.83×	0.88×	n/a	n/a	

Fold changes in blue were measured by SRI as part of this study.

well as with dose, with some biomarkers having little overlap in early days and others in later days. The PCA test statistic uses all three biomarkers on each day so that if any one (or more) of those biomarkers differ substantially from the distribution in normals, this indication of radiation exposure can be identified. The most relevant measure of the degree of overlap is the sensitivity and specificity of the PCA, both of which are quite high, as summarized in the AUC.

An important question is, to what extent are these markers confounded by other conditions or diseases. The Qiagen Ingenuity Pathway Analysis Database provides some helpful insight. Table 5 provides a listing of potentially confounding conditions obtained from the Ingenuity Database along with estimated prevalence (from the Centers for Disease Control and Prevention, CDC) and fold change for each condition. As can be seen from the table, in most cases, the condition is either rare in the general population or the fold change is much less than that observed in human TBI patients receiving 3.6 Gy of fractionated radiation. Some cases may require further investigation; for example, MCP1 levels may be elevated in individuals with inflammatory bowel disease or hypercholesterolemia. Future work will be required to collect relevant data on such population subgroups.

Conclusions

A radiation biodosimeter that can be used at the point of care to triage individuals who may have been exposed to ionizing radiation will have significant impact on the ability to provide timely and effective medical treatment and enable efficient use of scarce medical resources following a major nuclear event. Such a device should be capable of rapid detection of a panel of biomarkers that are indicative of absorbed radiation dose and provide a qualitative assessment of whether the individual received an absorbed dose of $\geq$2.0 Gy.

The plasma concentrations of the three radiation-responsive proteins identified in this research are sufficiently high that baseline levels can be detected using an optimized lateral flow test. Such tests are widely used for point-of-care diagnostics and would make an excellent assay platform for radiation exposure triage. In a subsequent paper, we will describe a device we have developed that can detect these proteins in a fingerstick blood sample with high accuracy and reliability.

Disclosure statement

The authors have no financial and/or business interest that may be affected by the research reported in this paper.

Funding

This work was funded in whole or in part with Federal funds from the Biomedical Advanced Research and Development Authority (BARDA), Office of the Assistant Secretary for Preparedness and Response, Office of the Secretary, Department of Health and Human Services, under Contract no. HHSSO10020100007C to SRI International.

Notes on contributors

Robert P. Balog received his PhD in BioMedical Engineering from the University of Texas, Southwestern Medical Center in 2004 and spent 14 years at SRI International as a program director. His research interests focus on the discovery of predictive in vitro diagnostic biomarkers and the development of distributed diagnostic platforms. Dr. Balog served as a Co-PI for this work.

Rowena Bacher received her MS in Biology from California State University, Fresno and specialized in biomarker discovery and developing novel immunoassays during her 8 years at SRI. Her current research interests focus on utilizing next-gen sequencing for pathogen detection.

Polly Chang received her Ph.D. in Biophysics from the University of California, Berkeley in 1991. She is currently the senior director of Molecular and Genetic Toxicology at SRI International and is actively engaged in the field of radiation biology coupled with product development of medical countermeasures for radiation protection. Dr. Chang served as a Co-PI for this work.

Michael Greenstein received his PhD in Physics from the University of Illinois-Champaign Urbana in 1981, and has worked on medical device since 1990, including ultrasound imaging, Immunoassay and Molecular Diagnostic systems. His research and development interests are focused on Point of Care medical devices.

Songeeta Jammalamadaka received her MS in Bioengineering from Tufts University and has worked at SRI since 2009 in the area of assay development and medical device engineering. She served as system engineer for writing requirements and specifications and is the lead usability researcher on this radiation biodosimeter project.

Songeeta Jammalamadaka received his PhD in Statistics from the University of California at Berkeley. He is a senior statistician at SRI International. His research interests include smoking cessation, biostatistics and educational studies.

Susan Knox received her Ph.D. in Microbiology from UC Davis and her MD from Stanford University. She did residency and fellowship training at Stanford and has been on the faculty there in Radiation Oncology since 1990.

Shirley Lee received her MS in Computer Science from Indiana University and has worked at SRI since 2011 in the area of bioinformatics and computational and statistical analysis methods with emphasis on classification and dynamic automation.

Hua Lin received her PhD in Chemistry from Fudan University (China) in 1989. She joined SRI in 2010 and is specialized for biomarker development. Her research interests are focused on proteomics and methodologies for ultra-sensitive sample analysis.

Thomas Shaler received his Ph.D. in Organic Chemistry from the University of California. His work at SRI International currently centers on the development of mass spectrometric analysis techniques for biological, biomedical and biotechnology applications.

Lei Shura received her MS in Neurosciences from Kent State University in 1998. She worked at Stanford University for 2 years as a Life Science Researcher and 6 years as a Clinical Research Coordinator. She managed multiple clinical studies with various phases in Radiation Oncology from start-up to close-out.

Paul Stein received his PhD in Cell and Developmental Biology from State University of New York, Stony Brook. He joined SRI International in 2010. His research interests focus on signaling pathways in inflammation and autoimmunity. He also directs immunoassay development to support various biomarker programs.

Kathryn Todd received her PhD in Physics from Stanford University in 2009 and has worked at SRI since 2010 as a research engineer, program manager, and associate laboratory director. Her research and development interests include Point of Care In Vitro Diagnostics, nanopore-based molecular diagnostics, and two-dimensional materials.

David E. Cooper received his PhD in Physics from MIT in 1980 and has worked in the area of medical devices, biosensors, and molecular diagnostics since 1996. Dr. Cooper served as the PI for this work.

References

Barrett A, Jacobs A, Kohn J, Raymond J, Powles RL. 1982. Changes in serum amylase and its isoenzymes after whole body irradiation. Br Med J (Clin Res Ed). 285:170–171.

Balog RP, Chang P, Javitz H, Lee S, Lin H, Shaler T, Cooper DE. 2018. Development of a point-of-care radiation biodosimeter: studies using novel protein biomarker panels in non-human primates. To be published this issue.

Bazan JG, Chang P, Balog R, D'Andrea A, Shaler T, Lin H, Lee S, Harrison T, Shura L, Schoen L, et al. 2014. Novel human radiation exposure biomarker panel applicable for population triage. Int J Radiat Oncol Biol Phys. 90:612–619.

Bertho JM, Demarquay C, Frick J, Joubert C, Arenales S, Jacquet N, Sorokine-Durm I, Quang Chau Q, Lopez M, Aigueperse J, et al. 2001. Level of Flt3-ligand in plasma: a possible new bio-indicator for radiation-induced aplasia. Intern J Radiat Biol. 77:703–712.

Bertho JM, Roy L, Souidi M, Benderitter M, Gueguen Y, Lataillade JJ, Prat M, Fagot T, De Revel T, Gourmelon P. 2008. New biological indicators to evaluate and monitor radiation-induced damage: an accident case report. Radiat Res. 169:543–550.

Bertho JM, Roy L, Souidi M, Benderitter M, Bey E, Racine R, Fagot T, Gourmelon P. 2009. Initial evaluation and follow-up of acute radiation syndrome in two patients from the Dakar accident. Biomarkers. 14: 94–102.

Buddemeier B. 2015. Medical needs in the aftermath of nuclear terrorism. LLNL-PRES-677346 (Presented at EPR BioDose 2015, Hanover, NH, October 48, 2015).

Buddemeier BR. 2011. National capital region: Key response planning factors for the aftermath of nuclear terrorism. Lawrence Livermore National Lab.(LLNL), Livermore, CA (United States). Report No: LLNL-TR-512111. Available from: http://fas.org/irp/agency/dhs/fema/ncr.pdf.

Citrin DE, Hitchcock YJ, Chung E, Frandsen J, Urick M, Shield W, Gaffney D. 2012. Determination of cytokine protein levels in oral secretions in patients undergoing radiotherapy for head and neck malignancies. Radiat Oncol. 7:64. doi: 10.1186/1748-717X-7-64.

Deshmane SL, Kremlev S, Amini S, Sawaya BE. 2010. Monocyte chemoattractant protein-1 (MCP-1): an overview. J Interferon Cytokine Res. 29:313–326.

Dressman HK, Muramoto GG, Chao NJ, Meadows S, Marshall D, Ginsburg GS, Nevins JR, Chute JP. 2007. Gene expression signatures that predict radiation exposure in mice and humans. PLoS Med. 4:e106.

Fisher RA. 1925. Statistical Methods for Research Workers. Oliver and Boyd (Edinburgh). ISBN 0-05-002170-2.

Gaugler M-H, Vereycken-Holler V, Squiban C, Vandamme M, Vozenin-Brotons M-C, Benderitter M. 2005. Pravastatin limits endothelial activation after irradiation and decreases the resulting inflammatory and thrombotic responses. Radiat Res. 163:479–487.

Guipaud O, Benderitter M. 2009. Protein biomarkers for radiation exposure: towards a proteomic approach as a new investigation tool. Ann Ist Super Sanita. 45:278–286.

Junglee D, Katrak A, Mohiuddin J, Blacklock H, Prentice HG, Dandona P. 1986. Salivary amylase and pancreatic enzymes in serum after total body irradiation. Clin Chem. 32:609–610.

Kenins L, Gill JW, Boyd RL, Holländer GA, Wodnar-Filipowicz A. 2008. Intrathymic expression of Flt3 ligand enhances thymic recovery after irradiation. J Exp Med. 205:523–531.

Kishima HK, Kirkham WR, Andrews JR. 1965. Post irradiation sialadenitis. A study of the clinical features, histopathologic changes and serum enzyme variations following irradiation of human salivary glands. Am J Roentgenol Radium Ther Nucl Med. 94:271–291.

Leslie MD, Dische S. 1992. Changes in serum and salivary amylase during radiotherapy for head and neck cancer: a comparison of conventionally fractionated radiotherapy with CHART. Radiother Oncol. 24:27–31.

Moriconi F, Christiansen H, Raddatz D, Dudas J, Hermann RM, Rave-Fränk M, Sheikh N, Saile B, Hess CF, Ramadori G. 2008. Effect of radiation on gene expression of rat liver chemokines: in vivo and in vitro studies. Radiat Res. 169:162–169.

Nalla AK, Gogineni VR, Gupta R, Dinh DH, Rao JS. 2011. Suppression of uPA and uPAR blocks radiation-induced MCP-1 mediated recruitment of endothelial cells in meningioma. Cell Signal. 23:1299–1310.

Port M, Majewski M, Herodin F, Valente M, Drouet M, Forcheron F, Tichy A, Sirak I, Zavrelova A, Malkova A, et al. 2018. Validating baboon ex vivo and in vivo radiation-related gene expression with corresponding human data. Radiat Res. 189:389–398.

Siva S, MacManus M, Kron T, Best N, Smith J, Lobachevsky P, Ball D, Martin O. 2014. A pattern of early radiation-induced inflammatory cytokine expression is associated with lung toxicity in patients with non-small cell lung cancer. PLoS One. 9:e109560.